Synthesis of Multiple Beam Linear Arrays with Uniform Amplitudes

Aslan, Yanki; Puskely, Jan; Roederer, Antoine; Yarovoy, Alexander

DOI
10.1049/cp.2018.0422

Publication date
2018

Document Version
Final published version

Published in
Proceedings - 12th European Conference on Antennas and Propagation, EUCAP 2018

Synthesis of Multiple Beam Linear Arrays with Uniform Amplitudes

Yanki Aslan[1], Jan Puskely[2], Antoine Roederer[3], Alexander Yarovoy[4]
MS3 Group, Department of Microelectronics, Faculty of EEMCS
Delft University of Technology
Mekelweg 4, 2628 CD Delft, the Netherlands
{[1]Y.Aslan, [2]J.Puskely-1, [3]A.G.Roederer, [4]A.Yarovoy}@tudelft.nl

***Abstract*—A convex iterative algorithm for the synthesis of uniform amplitude, space-tapered linear phased arrays with simultaneous multiple beam optimization for 5G applications is presented. The performance of the algorithm is demonstrated by the synthesis of two arrays having 16 and 24 elements with 60 and 90 degree scan range, respectively. The effect of phase shifter quantization is also addressed. The results indicate that the space-tapered arrays with multiple beam optimization have improved radiation performance in terms of the side lobe level when compared to both single, broadside, beam optimized space-tapered arrays and uniformly distributed arrays with half wavelength spacing.**

***Index Terms*—linear antenna arrays, phased arrays, antenna synthesis, space taper, density taper, multibeam optimization, convex optimization, 5G communications.**

I. Introduction

To meet ambitious 5G system requirements, new approaches for wide-angle scanning antenna arrays with low level of side lobes and acceptable power amplifier efficiencies are required.

Amplitude, phase and position optimization are common antenna array synthesis techniques that are used to approximate a certain current distribution on an aperture depending on a desired radiation pattern. In amplitude and phase optimization, the positions of antennas are fixed while the weights are adjusted in order to satisfy the radiation requirements. On the other hand, in position optimization, the weights are kept uniform and the element locations are modified, which is named as space (or density) tapering. Apart from its practical interest, the main advantage of space tapering is that since the array is excited uniformly, the amplifiers powering the array can all work at the same, power-efficient working point with reduced co-channel interference [1]–[3].

A large variety of uniform amplitude array synthesis methods exist in the literature. Many global optimization algorithms [4]–[7] have been used successfully to design directive arrays with low side lobes. However, the computational burden of such methods increases rapidly with the number of antenna elements. To overcome this limitation, deterministic synthesis techniques [8]–[11] have been developed. Despite their higher computational efficiency and superior performance compared to the global optimization tools, these techniques have larger analytical complexity and may require a properly chosen continuous source acting as a reference to be emulated.

Array synthesis via convex optimization methods was first introduced in [12] as an easy-to-implement, computationally effective and efficient alternative to the existing approaches. Recently, sparsity-based convex optimization methods [13], [14] have been widely used in aperiodic array synthesis which are also able to take into account the effect of mutual coupling [15] and joint optimization for multiple beams [16]. In fact, these are two important aspects that are often wrongly neglected. Mutual coupling may significantly affect the embedded element patterns, and thus the radiation pattern, especially for closely spaced elements and single (broadside) beam optimization may cause a significant performance degradation in terms of side lobe levels while scanning the beam off-broadside.

Although able to address these issues, the mentioned sparsity-based convex methods apply both amplitude and space tapering to the elements. Besides, there is no control over the minimum element spacing, which may result in impractical inter-element distances in the final layout.

In [17], an iterative convex optimization technique has been proposed to synthesize uniform amplitude, space-only tapered linear and planar arrays. The aim was to optimize the locations of a fixed number of elements to form a broadside beam with low side lobes. The possibility of defining a minimum element spacing for linear arrays was mentioned, but not implemented.

Considering the work in [17] as a reference and motivated by the multiple beam optimization results presented in [16], we propose in this paper an original simultaneous multiple beam optimization procedure for the synthesis of uniform amplitude, space-tapered linear arrays with pre-defined minimum inter-element spacing. The formulation of the optimization problem is given in Section II. Synthesis results are presented in Section III. Section IV concludes the paper.

II. Formulation of the optimization problem

Let us consider an N-element uniformly excited linear array, whose geometry is given in Fig. 1.

The far field radiated by such an array is given by

$$f(\theta) = \sum_{n=1}^{N} E_n(\theta) e^{jk\cos\theta z_n} \tag{1}$$

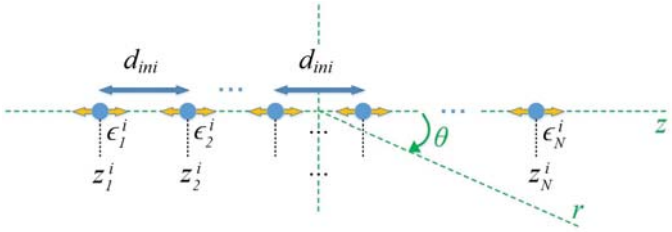

Fig. 1. Geometry of a linear array of N elements.

where $E_n(\theta)$ is the pattern of the n^{th} element. If the same isolated pattern, $E(\theta)$, is assumed for each element, the far field, $f(\theta)$ becomes

$$f(\theta) = E(\theta) \sum_{n=1}^{N} e^{jk\cos\theta z_n} \tag{2}$$

In the iterative convex optimization algorithm proposed in [17], the idea is to start from an initial, uniformly distributed array (with spacing d_{ini}) and move element n by ϵ_n^i at the i^{th} step of the algorithm, which gives

$$z_n^i = z_n^{i-1} + \epsilon_n^i \tag{3}$$

Inserting (3) into (2) and assuming the following relation holds

$$|k\cos\theta\epsilon_n^i| \ll 1,\ i.e.,\ |\epsilon_n^i| \ll \lambda/2\pi = 0.16\lambda \tag{4}$$

the far field expression can be linearized around the element locations using the Taylor expansion: $e^{j\phi} = 1 + j\phi$, where $\phi = k\cos\theta\epsilon_n^i$. Thus, the far field at the i^{th} iteration can be approximated by

$$f_{\epsilon_n}^i(\theta) \approx E(\theta) \sum_{n=1}^{N} e^{jk\cos\theta z_n^{i-1}} (1 + jk\cos\theta\epsilon_n^i) \tag{5}$$

Now, let us assume a scenario where the beam is scanned at p different angles. θ_{s_m} represents the direction of maximum radiation for the scanned beam $s_{m=1,2,\ldots,p}$. Then, the phase shift of the n^{th} element for the scan angle θ_{s_m} at the i^{th} iteration is given by

$$\Phi_{n,s_m}^i = e^{-jk\cos\theta_{s_m} z_n^i} \tag{6}$$

Using the same procedure while deriving the expression in (5), the far field of a scanned beam s_m at the i^{th} iteration can be computed as follows

$$f_{\epsilon_n}^{i,s_m}(\theta) \approx E(\theta) \sum_{n=1}^{N} e^{jk(\cos\theta - \cos\theta_{s_m}) z_n^{i-1}} (1 + jk\cos\theta\epsilon_n^i)(1 - jk\cos\theta_{s_m}\epsilon_n^i) \tag{7}$$

Discarding the higher-order terms in (7), the following approximation is obtained, which can be used at each iteration of the convex optimization algorithm

$$f_{\epsilon_n}^{i,s_m}(\theta) \approx E(\theta) \sum_{n=1}^{N} e^{jk(\cos\theta - \cos\theta_{s_m}) z_n^{i-1}} (1 + jk(\cos\theta - \cos\theta_{s_m})\epsilon_n^i) \tag{8}$$

Vectors of parameters that are used in the algorithm are defined as

$$\begin{aligned} \boldsymbol{z}^i &= \begin{bmatrix} z_1^i & z_2^i & \cdots & z_N^i \end{bmatrix}^T, \\ \boldsymbol{\epsilon}^i &= \begin{bmatrix} \epsilon_1^i & \epsilon_2^i & \cdots & \epsilon_N^i \end{bmatrix}^T, \\ \boldsymbol{\theta_s} &= \begin{bmatrix} \theta_{s_1} & \theta_{s_2} & \cdots & \theta_{s_p} \end{bmatrix}, \\ \boldsymbol{\Theta_{SL,s}} &= \begin{bmatrix} \boldsymbol{\theta_{SL,s_1}} & \boldsymbol{\theta_{SL,s_2}} & \cdots & \boldsymbol{\theta_{SL,s_p}} \end{bmatrix} \end{aligned} \tag{9}$$

where $\boldsymbol{z}^i$ and $\boldsymbol{\epsilon}^i$ contain the locations and position shifts at i_{th} iteration, respectively. Scan angles used in the optimization form $\boldsymbol{\theta_s}$. $\boldsymbol{\theta_{SL,s_m}}$ is a vector containing vectors of angles forming the side lobe region for each scan angle. These regions are determined according to a pre-specified beam width, θ_b such that

$$\theta \in \boldsymbol{\theta_{SL,s_m}}\ if\ \theta < (\theta_{s_m} - \theta_b)\ or\ \theta > (\theta_{s_m} + \theta_b) \tag{10}$$

In order to calculate the resulting inter-element spacings at each iteration, an $(N-1) \times N$ circulant matrix, D, is formed as follows

$$D = \begin{bmatrix} -1 & 1 & 0 & 0 & \cdots & 0 & 0 & 0 \\ 0 & -1 & 1 & 0 & \cdots & 0 & 0 & 0 \\ 0 & \ddots & \ddots & \ddots & \ddots & \ddots & \ddots & \vdots \\ \vdots & \ddots & \ddots & \ddots & \ddots & -1 & 1 & 0 \\ 0 & 0 & 0 & 0 & 0 & 0 & -1 & 1 \end{bmatrix} \tag{11}$$

Considering the field expression in (8) and the formulations in (9), (10) and (11), the convex problem to be solved at the i^{th} iteration of the algorithm is formulated as follows

$$\min_{\boldsymbol{\epsilon}^i} \rho, \quad s.t. \begin{cases} \max |f_{\boldsymbol{\epsilon}^i}^{i,\boldsymbol{\theta_s}}(\boldsymbol{\Theta_{SL,s}})| \le \rho \\ |\boldsymbol{\epsilon}^i| \le \mu \\ D^*(\boldsymbol{\epsilon}^i + \boldsymbol{z}^{i-1}) \ge d_{\min} \end{cases} \tag{12}$$

where ρ is the maximum side lobe level which is simultaneously minimized for all the defined scan angles, $\boldsymbol{\theta_s}$. $|\boldsymbol{\epsilon}^i|$ is upper-bounded by a user-defined constant μ, as in (4). The last constraint guarantees that the minimum inter-element spacing at each iteration is larger than or equal to a desired value, $d_{\min}$.

III. Synthesis Results

The algorithm is first tested for two example cases using 16 and 24 element linear antenna arrays with ± 30 and ± 45 degree scan angle range, respectively. A convergence analysis is then performed by observing the maximum side lobe level at each iteration. The effect of varying the upper-bound of position shifts, μ and the initial inter-element spacing, d_{ini} on the

convergence is also studied for the 24-element array. Lastly, the influence of phase shifter quantization on the side lobe levels is investigated by using 6-bit and 4-bit phase shifters and rounding the element phase values appropriately.

A. Optimization for Multiple Beams

Simultaneous multiple beam optimization is performed for two example antenna arrays having 16 and 24 elements. In both cases, an isolated element pattern $E(\theta) = \sin\theta$ is assumed, which is in line with [17]. The initial inter-element spacing is equal to 0.5λ, i.e. $d_{ini} = 0.5\lambda$. To limit high mutual coupling effects, the minimum inter-element spacing is set to half wavelength, i.e. $d_{\min} = 0.5\lambda$. The upper bound for position shifts, μ, is equal to 0.16λ and the observation angle, θ, is discretized with 0.5 degree steps. For the 16-element array, θ_b is equal to 8 degrees and the beam is scanned in ± 30 degree range with 10 degree steps, while for 24-element array, θ_b is equal to 5 degrees and the beam is scanned in ± 45 degree range with 15 degree steps. In Fig. 2 and Fig. 3, radiation pattern comparison of single (broadside) beam (SB) optimization and multiple beam (MB) optimization results are shown for 16-element and 24-element arrays, respectively. Table I shows the resulting element positions for the 16-element space-tapered arrays.

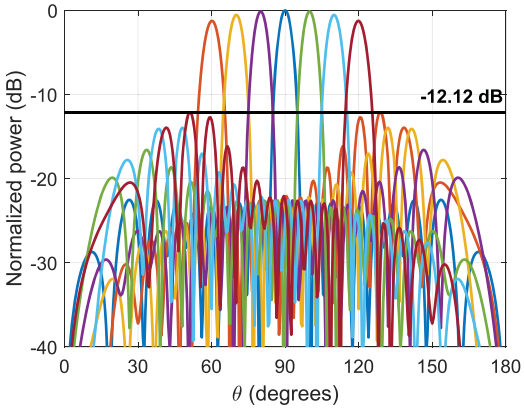

(a)

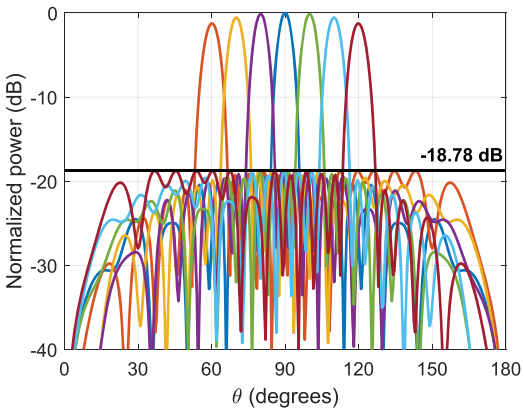

(b)

Fig. 2. Far-field pattern of a 16-element space-tapered array, (a) single (broadside) beam optimization, (b) multiple beam optimization in ± 30 degrees; θ_b = 8 degrees, μ = 0.16λ, d_{ini} = 0.5λ, $d_{\min}$ = 0.5λ

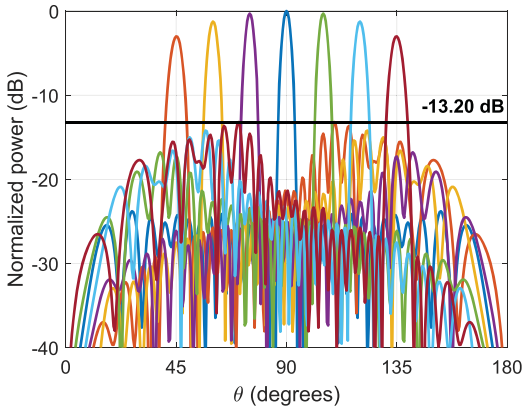

(a)

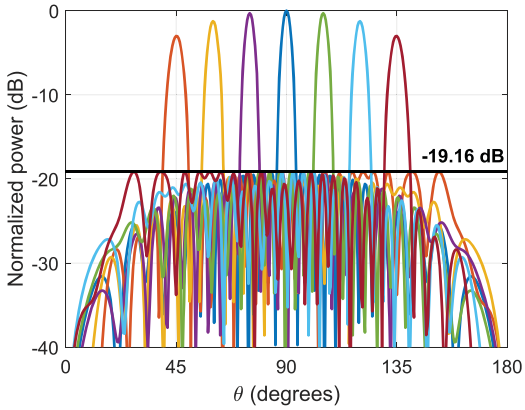

(b)

Fig. 3. Far-field pattern of a 24-element space-tapered array, (a) single (broadside) beam optimization, (b) multiple beam optimization in ± 45 degrees; θ_b = 5 degrees, μ = 0.16λ, d_{ini} = 0.5λ, $d_{\min}$ = 0.5λ

TABLE I
ANTENNA LOCATIONS OF THE 16-ELEMENT LINEAR ARRAY FOR SINGLE BEAM (SB) AND MULTIPLE BEAM (MB) OPTIMIZATION

n	z_n/λ-*SB*	z_n/λ-*MB*	n	z_n/λ-*SB*	z_n/λ-*MB*
1	-4.93	-4.53	9	0.26	0.47
2	-3.84	-3.74	10	0.77	0.97
3	-3.09	-2.73	11	1.27	1.47
4	-2.39	-2.19	12	1.81	2.02
5	-1.81	-1.56	13	2.38	2.65
6	-1.24	-1.03	14	3.05	3.25
7	-0.74	-0.53	15	3.99	3.95
8	-0.24	-0.03	16	4.87	4.49

The proposed method provides lower side lobe levels compared to the single beam optimization while scanning the beam off-broadside. For the given input parameters (element pattern, scan range, beamwidth, minimum spacing etc.), the reductions in the maximum side lobe level for the 16 and 24-element arrays are 6.66 dB and 5.96 dB, respectively.

B. Convergence Analysis

Convergence of the multiple beam optimization algorithm results given in Fig. 2(b) and Fig. 3(b) is shown next in Fig. 4, where the maximum side lobe level is plotted at each iteration, starting from the uniformly distributed array spaced with half wavelength.

For both arrays, convergence is achieved after 15-20 iterations. Compared to the uniform layouts with 0.5λ spacing, the maximum side lobe levels within the respective scan ranges are decreased by 5.60 dB and 5.86 dB for the 16 and 24-element arrays, respectively. The improvement in side lobe level is achieved at the expense of increased array length due to space tapering. The array lengths after optimization become 9.02λ and 13.71λ for 16 and 24-element arrays, respectively.

The convergence with varying μ is plotted for 24-element array in Fig. 5. The result indicates the minimum side lobe level achieved by the algorithm is robust to the choice of the upper-bound. However, faster convergence is observed for larger μ, which validates the selection in Section III-A.

Lastly, the effect of selecting different initial inter-element spacing, d_{ini}, on the convergence is studied. Fig. 6 shows the maximum side lobe level at each iteration for the 24-element array with $\mu = 0.16\lambda$ and $d_{\min} = 0.5\lambda$ for various d_{ini}. Slight improvement (about 0.2 dB) is obtained in the maximum side lobe level when 0.6λ spacing is used instead of 0.5λ, while the convergence point gets higher for larger d_{ini}.

C. Phase Shifter Quantization Effect

Quantized phase shifters affect the phase shift values applied at each element while scanning the beam, which alters the radiation pattern. In this work, the resulting phase shifts found by the algorithm are rounded to the closest available phase values to observe the effect of quantization. Fig. 7 shows the array patterns with continuous, 6-bit and 4-bit phase shifters for the 24-element array with the "optimal" input parameters found in Section III-A and Section III-B ($\mu = 0.16\lambda$ and $d_{ini} = 0.6\lambda$).

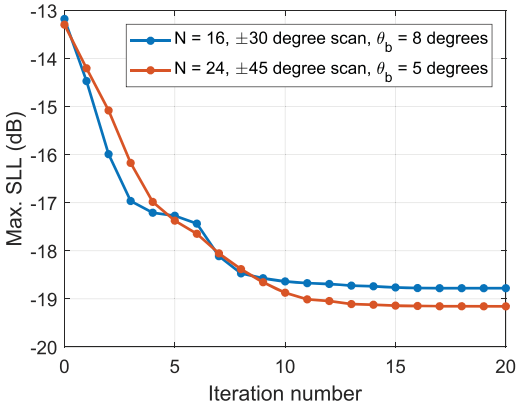

Fig. 4. Convergence analysis of multiple beam optimization algorithm for 16 and 24 element space-tapered arrays; $\mu = 0.16\lambda$, $d_{ini} = 0.5\lambda$, $d_{\min} = 0.5\lambda$

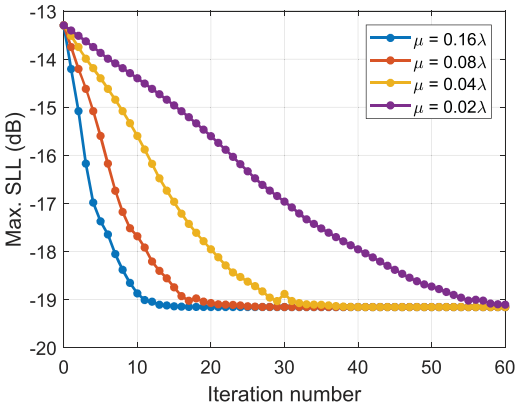

Fig. 5. Convergence for various upper bounds, μ, for the 24-element array; $\theta_b = 5$ degrees, $d_{ini} = 0.5\lambda$, $d_{\min} = 0.5\lambda$

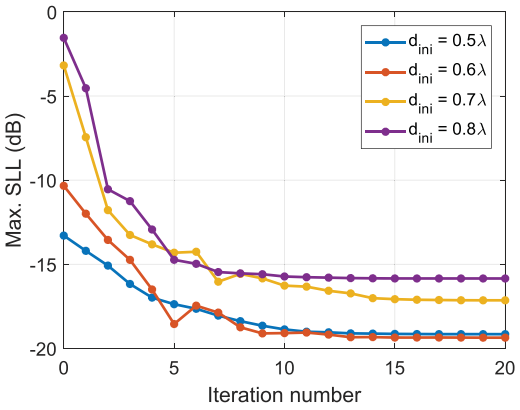

Fig. 6. Convergence for various initial inter-element spacings, d_{ini}, for the 24-element array; $\theta_b = 5$ degrees, $\mu = 0.16\lambda$, $d_{\min} = 0.5\lambda$

Due to quantization of phase shifts, the maximum side lobe levels increase by 0.52 dB and 2.01 dB for 6-bit and 4-bit phase shifters, respectively.

All numerical computations have been carried out on an Intel(R) Core(TM) i7-4710HQ 2.5GHz CPU, 16GB RAM computer. Each iteration takes about 3-4 seconds.

IV. Conclusion

A uniform amplitude, space-tapered linear array synthesis method has been proposed for phased arrays that are suitable for 5G applications.

The iterative convex optimization technique used in [17] has been extended to simultaneous multiple beam optimization with an option to pre-define the desired minimum inter-element spacing in the final layout.

The algorithm performance has been demonstrated using 16 and 24-element arrays having ±30 and ±45 degree scan angle range, respectively. Compared to the single beam optimization, maximum side lobe level has been reduced by around 6-7 dB for the optimized array topologies. Besides, compared to uniformly distributed array with half wavelength spacing,

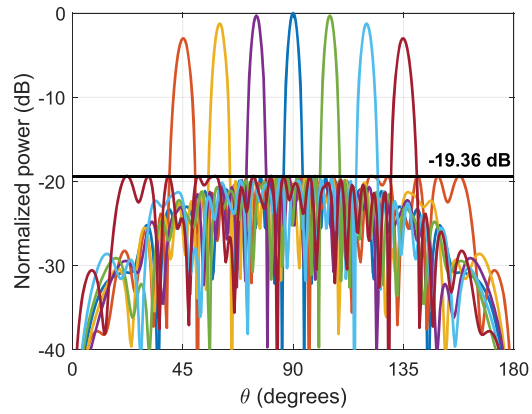

(a)

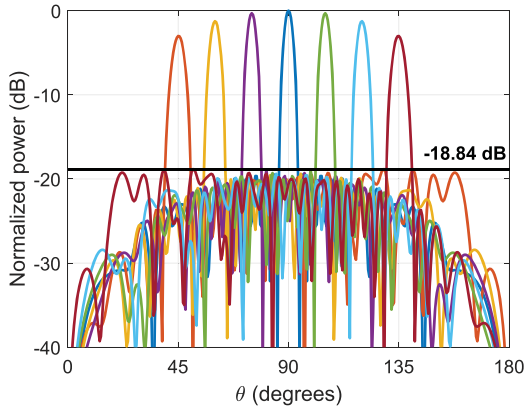

(b)

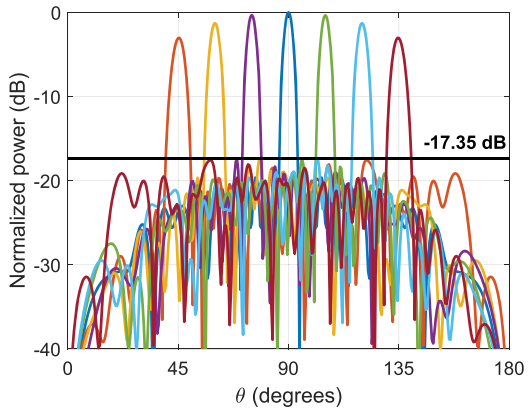

(c)

Fig. 7. Effect of quantized phase shifters on the far-field pattern of the 24-element space-tapered array with multiple beam optimization, (a) continuous phase, (b) 6-bit phase shifter, (c) 4-bit phase shifter; θ_b = 5 degrees, μ = 0.16λ, d_{ini} = 0.6λ, $d_{\min}$ = 0.5λ

the resulting space-tapered, multiple beam optimized arrays have provided around 5.5-6 dB suppression in the maximum side lobe level within their respective scan ranges, but at the expense of increased array lengths about 20%.

Finally, the effect of quantized phase shifters has been also studied for the 24-element array by rounding the phase shift of each element to the closest available phase value. For 6-bit and 4-bit phase shifters, the maximum side lobe level in $\pm$45 degree scan range has increased by approximately 0.5 dB and 2 dB, respectively.

ACKNOWLEDGMENT

This research was conducted as part of the STW-NXP Partnership Program on Advanced 5G Solutions within the project titled “Antenna Topologies and Front-end Configurations for Multiple Beam Generation”. For further information: www.nwo.nl.

REFERENCES

[1] R. E. Willey, “Space tapering of linear and planar arrays,” *IRE Trans. Antennas Propag.*, vol. 10, no. 4, pp. 369-377, Jul. 1962.

[2] S. S. Kuo, G. P. Junker, T. K. Wu and C. H. Chen, “A density taper technique for low side lobe applications of hex array antennas,” in *Proc. IEEE Int. Conf. Phased Array Syst. Technol., 2000*, pp. 493-496, Dana Point, CA, USA, May 2000.

[3] G. Toso, P. Angeletti and C. Mangenot, “A comparison of density and amplitude tapering for transmit active arrays,” in *Proc. 3rd EuCAP*, pp. 840-843, Berlin, Germany, Mar. 2009.

[4] D. G. Kurup, M. Himdi and A. Rydberg, “Synthesis of uniform amplitude unequally spaced antenna arrays using the differential evolution algorithm,” *IEEE Trans. Antennas Propag.*, vol. 51, no. 9, pp. 2210-2217, Sep. 2003.

[5] K. Chen, Z. He and C. Han, “A modified real GA for the sparse linear array synthesis with multiple constraints,” *IEEE Trans. Antennas Propag.*, vol. 54, no. 7, pp. 2169-2173, Jul. 2006.

[6] N. Jin and Y. Rahmat-Samii, “Advances in Particle Swarm Optimization for Antenna Designs: Real-Number, Binary, Single-Objective and Multi-objective Implementations,” *IEEE Trans. Antennas Propag.*, vol. 55, no. 3, pp. 556-567, Mar. 2007.

[7] H. Oraizi and M. Fallahpour, “Nonuniformly spaced linear array design for the specified beamwidth/sidelobe level or specified directivity/sidelobe level with coupling considerations,” *Prog. Electromagn. Res. M*, vol. 4, pp. 185-209, 2008.

[8] M. I. Skolnik, “Nonuniform arrays,” in *Antenna Theory*, R. E. Colin and F. J. Zucker, Eds. New York: McGraw-Hill, 1969, ch. 6, pt. 1.

[9] O. M. Bucci, M. D’Urso, T. Isernia, P. Angeletti and G. Toso, “Deterministic synthesis of uniform amplitude sparse arrays via new density taper techniques,” *IEEE Trans. Antennas Propag.*, vol. 58, no. 6, pp. 1949-1958, Jun. 2010.

[10] M. C. Vigano and D. Caratelli, “Analytical synthesis technique for uniform-amplitude linear sparse arrays,” in *IEEE AP-S / URSI Symp.*, Toronto, Canada, Jul. 2010.

[11] A. F. Morabito, T. Isernia and L. Di Donato, “Optimal synthesis of phase-only reconfigurable linear sparse arrays having uniform-amplitude excitations,” *Prog. Electromagn. Res.*, vol. 124, pp. 405-423, 2012.

[12] H. Lebret and S. Boyd, “Antenna pattern synthesis via convex optimization,” *IEEE Trans. Signal Process.*, vol. 45, no. 3, pp. 526-531, Mar. 1997.

[13] S. E. Nai, W. Ser, Z. L. Yu and H. Chen, “Beampattern synthesis for linear and planar arrays with antenna selection by convex optimization,” *IEEE Trans. Antennas Propag.*, vol. 58, no. 12, pp. 3923-3930, Dec. 2010.

[14] G. Prisco and M. D’Urso, “Maximally sparse arrays via sequential convex optimization,” *IEEE Antennas Wireless Propag. Lett.*, vol. 11, pp. 192-195, Feb. 2012.

[15] C. Bencivenni, M. V. Ivashina, R. Maaskant and J. Wettergren, “Design of maximally sparse antenna arrays in the presence of mutual coupling,” *IEEE Antennas Wireless Propag. Lett.*, vol. 14, pp. 159-162, Sep. 2014.

[16] C. Bencivenni, M. V. Ivashina, R. Maaskant and J. Wettergren, “Synthesis of maximally sparse arrays using compressive sensing and full-wave analysis for global earth coverage applications,” *IEEE Trans. Antennas Propag.*, vol. 64, no. 11, pp. 4872-4877, Jul. 2016.

[17] B. Fuchs, A. Skrivervik and J R. Mosig, “Synthesis of uniform amplitude focused beam arrays,” *IEEE Antennas Wireless Propag. Lett.*, vol. 11, pp. 1178-1181, Oct. 2012.